

THE ROLE OF THE STRUCTURAL CHARACTERISTIC LENGTH IN FRC STRUCTURES

MARCO DI PRISCO^{*}, MATTEO COLOMBO[†] AND ISABELLA G. COLOMBO^{††}

Politecnico di Milano
Milano, ITALY

^{*} e-mail: marco.diprisco@polimi.it

[†] e-mail: matteo.colombo@polimi.it

^{††} e-mail: isabellagiorgia.colombo@polimi.it

Key words: Fiber reinforced concrete, Bending, Crack spacing, Structural characteristic length, Thin-walled elements.

Abstract: In the framework of the CEN Committee involved in the writing of the fiber reinforced concrete structure standards, a strong debate has been focused on the possibility to use a stress-strain rather than a stress- crack opening constitutive relationship, even if only the second one is physically meaningful after the cracking of the matrix. The use of a stress-strain model, even if it can be regarded as an effective simplification in many cases as it is in R/C structures, can be justified by the rough choice of a unique crack spacing in the range of 125 mm.

In the paper, the modeling of different FRC cross sections and in particular of a thin-walled open cross-section profile longitudinally reinforced with steel bars like a FRC box-culvert (U-channel) highlights as only the use of a correct structural characteristic length when a simplified Navier-Bernoulli plane section model is adopted prevents the overestimation of the bearing capacity in bending. A comparison with F.E. model and previous experimental tests on full-scale structures are also proposed.

1 INTRODUCTION

Fiber reinforced concrete is characterised by a significant residual toughness in the post-cracking regime. The simplest mechanical approach to take into account this property is the identification of a stress-crack opening constitutive law in uniaxial tension, assuming the material as a composite that can be regarded as isotropic if fibre distribution is not affected by special executing factors like wall effects or casting procedures. The pull-out contribution, that is activated only after crack

opening takes place, forces the designer to introduce a structural characteristic length depending on the particular kinematic model used in the investigation. If plane section approach is used, the structural characteristic length is mainly correlated to crack spacing. If a Finite Element approach is adopted, often the rules introduced in the algorithms, calibrated for plain concrete, cannot be simply extended to FRC because they can introduce an overestimation of the dissipated energy due to the progressive increase of the crack band also

in case of softening behaviour.

2 REFERENCE CASES

The choice of the structural characteristic length of a fiber reinforced concrete member is strictly related to the crack spacing of the element itself.

In this Section, some meaningful examples - useful for the definition of the crack spacing in the following Sections of the paper - are given.

Concerning bent R/C elements with a not homogeneous reinforcement, a significant example is given by Leonhardt [1]. He showed the crack pattern of a T beam, in which the zone of the bottom chord strongly reinforced ($4 \phi 26$ mm) presents a small crack spacing and corresponding small crack widths; on the contrary, outside this zone, the weak web reinforcement cannot prevent wide cracks originated by larger crack spacing (Figure 1).

Another interesting example on the same subject is given by di Prisco et al. [2]. Looking at the crack pattern of a HPSFRC roof element (Figure 2), it is possible to note that the crack spacing is smaller in the prestressed chords, rather than in the flat bottom slab, which is reinforced simply with fibers (no traditional steel reinforcement) and it is mainly subjected to tensile stresses. Due to the softening behavior in uniaxial tension of the FRC used, the crack spacing in the bottom flat slab is related to the slab width (equal to about 0.83 m).

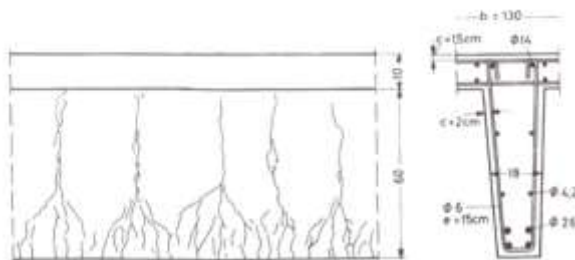


Figure 1: Crack pattern of a T beam [1].

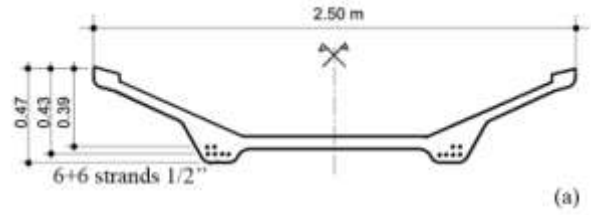


Figure 2: HPSFRC prestressed roof element: cross-section (a) and crack pattern (b) [2].

In case of deflection hardening materials and sections subjected to bending, the crack distance is related to the thickness of the bent element (Figure 3 [3]) as it occurs in plane beams subjected to a modest eccentric compression.

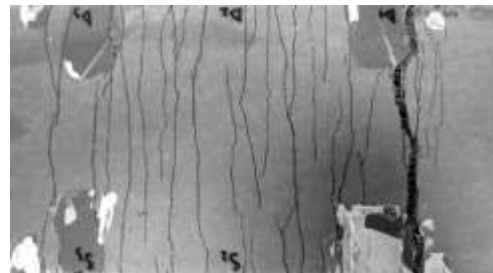
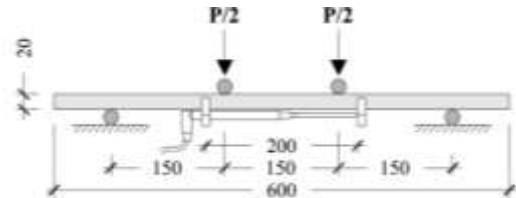


Figure 3: HPFRC plate 150 mm wide: four point bending test set-up (a) and crack pattern on the bottom face (b) [3].

3 SHALLOW BEAM: RELIABILITY OF THE USE OF A UNIQUE CHARACTERISTIC LENGTH

If a structural element is characterized by a section in which different structural characteristic lengths can be identified, the use of only one characteristic length in the prediction of the behavior is reliable when these characteristic lengths vary in a limited range.

To assess the truthfulness of this assertion, a fiber reinforced shallow beam cast in a prefabrication plant and tested at Politecnico di Milano is taken as a reference [4]. The beam is 1600 mm long and it is characterized by a rectangular cross-section 500 mm wide and 125 mm thick. It is reinforced with polypropylene fibers and a minimum steel reinforcement made of 4+4 Φ 6 longitudinal steel bars and Φ 6/10 stirrups is provided (Figure 4). A four point bending test was performed on the beam considering a distance between the supports equal to 1400 mm and a lever arm of 500 mm.

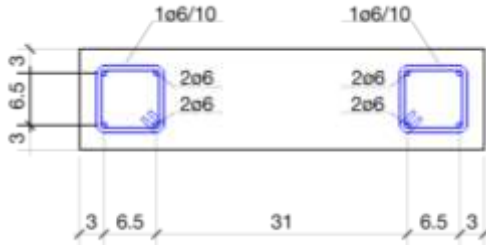


Figure 4: Shallow beam cross-section (measures in cm).

3.1 Materials

The shallow beam is made of polypropylene fiber reinforced concrete. According to MC2010 [5] the concrete used to cast the beam can be classified as “C35- 2e”. The properties, defined according to MC2010, are summarized in Table 1. In particular the Young’s modulus (E_{ci}), the characteristic compressive strength (f_{ck}), the average compressive strength (f_{cm}) and the lower bound value of characteristic tensile strength (f_{ctk}) are collected.

Table 1: Properties of concrete class “C35”

E_{ci} [MPa]	f_{ck} [MPa]	f_{cm} [MPa]	f_{ctk} [MPa]
35000	35	43	2.2

The tensile properties of FRC were determined testing twelve specimens cured for 32 days following the procedure shown in MC2010 (Figure 5.6-5) referred to EN14651 [6]. The results are collected in Table 2 in terms of limit of proportionality f_L and residual tensile strengths f_{R1} and f_{R3} , which respectively correspond to a crack mouth opening displacement ($CMOD$) of 0.5 and 2.5 mm. Both average and characteristic values are collected in the Table; the latter values were computed starting from average values according to the formula proposed in EN1990 [7] considering a log-normal distribution and an un-known coefficient of variation V_x .

Table 2: Tensile properties of FRC

	f_L [MPa]	f_{R1} [MPa]	f_{R3} [MPa]
f_{av}	5.05	3.52	5.54
f_k	4.35	2.14	3.21

Yield stress f_y , ultimate strength f_t and elongation A_{gt} of steel reinforcing bars are collected in Table 3. Characteristic values were computed starting from average values according to EN1990 considering a normal distribution and an un-known coefficient of variation V_x .

Table 3: Properties of steel rebars

	f_y [MPa]	f_t [MPa]	A_{gt} [-]
av	559	590	0.045
k	550	577	0.039

3.2 Constitutive laws used in the prediction

Concerning concrete in compression, a parabolic-rectangular stress-strain relationship is adopted; the maximum strength f_c is reached at a compressive strain equal to $2e-3$, while the failure occurs at a strain of $3.5e-3$ (MC2010 - Figure 7.2-8 and Equations 7.2-13 and 7.2-14).

A linear pre-cracking and linear post-cracking constitutive law is used to model the FRC behavior in tension.

According to di Prisco et al. [8], the linear post-cracking stress-*CMOD* behavior is identified through two points:

($CMOD = 0.5 \text{ mm}; \sigma = 0.37 f_{R1}$) and
 ($CMOD = 2.5 \text{ mm}; \sigma = 0.5 f_{R3} - k_b/2 f_{R1}$),
 with $k_b = 0.529 - 0.143 f_{R3}/f_{R1}$.

According to MC2010, for bent elements the maximum value of crack opening displacement (w_u) has to be limited to the minimum value between 2.5 mm and $0.02 l_{cs}$, where l_{cs} represents the structural characteristic length of the element.

The stress-strain relationship is obtained starting from the stress-*CMOD* curve by dividing the *CMOD* by the structural characteristic length (l_{cs}) of the element portion.

The characteristic length is computed as the minimum value between the mean distance between cracks s_{rm} and the distance y between the neutral axis and the tensile side of the cross-section (see Eq. 5.6-8, MC2010). s_{rm} can be taken equal to 1.5 times the length over which slip between concrete and steel occurs (MC2010 - Equation 7.6-4, modified in 7.7-23).

Two cases are considered: the introduction of two characteristic lengths (one for the central part of the specimen, reinforced just with fibers, and another one for the lateral parts, reinforced with both fibers and steel bars) and the introduction of just one characteristic length for the whole section.

When two characteristic lengths are introduced, the values used are defined as follows. The central part of the specimen is loaded in bending and does not present traditional reinforcement; hence, according to MC2010, it is possible to assume $y = h = 125 \text{ mm}$. In the lateral parts the concrete is reinforced with traditional steel rebars, hence the characteristic length is assumed equal to the lower value between $y = 95 \text{ mm}$ and $s_{rm} = 95 \text{ mm}$; hence, it is equal to 95 mm.

When one characteristic length is introduced, it is computed considering all the section as reinforced with steel bars. Hence, it is chosen as the lower value between $y = 102 \text{ mm}$ and $s_{rm} = 152 \text{ mm}$ (which is 102 mm).

The behavior of steel rebars is idealized through a bi-linear elasto-plastic stress-strain diagram, assuming a Young's modulus of 206 GPa and accounting the mechanical properties previously summarized in Table 3.

3.3 Comparison between experimental and analytical results

Following a plane section approach, bending moment vs. curvature diagrams collected in Figure 5 are obtained considering both characteristic (k) and mean (m) material values, for both the cases in which one or two characteristic lengths are taken into account. All the analytical curves are drawn up to the point at which w_u is reached.

In the same graph the experimental curve is plotted in order to validate the prediction. Note that the experimental curve is arrested before the peak, to preserve the LVDT transducers. The bending moment at which failure occurred is represented in the graph through a dashed line.

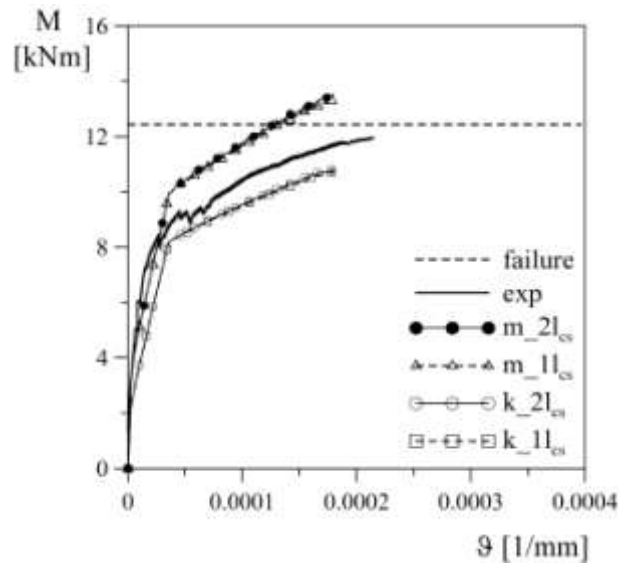


Figure 5: Shallow beam sectional behavior: bending moment vs. curvature diagrams.

It is interesting to observe how in this case the introduction of two structural characteristic lengths is fully negligible because the range of variation is limited (95 - 125 mm) and therefore a unified structural characteristic length can be adopted.

4 U-CHANNEL: RELIABILITY OF THE USE OF THE RIGHT STRUCTURAL CHARACTERISTIC LENGTHS

In this Section, the modeling of a thin-walled open cross-section profile longitudinally reinforced with steel bars is proposed. The focus is placed on the different sectional responses obtained if one or more characteristic lengths are used in the model.

The geometry and the reinforcement of the culvert (U-channel) are shown in Figure 6. Proper concrete cover and bar spacing are provided in order to satisfy the MC2010 limitations. The section is reinforced providing the minimum area of steel reinforcement which allows to sustain, at the characteristic yield stress value, the load inducing the first cracking of concrete.

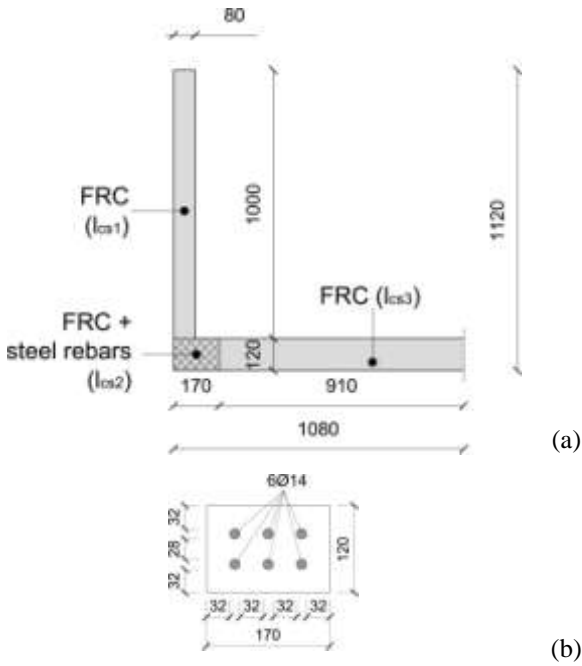


Figure 6: U-channel cross-section (measures in mm): half section (a) and detail of the part reinforced with steel bars (b).

4.1 Materials

As in the previous example, a concrete class “C35” is taken into account (see Table 1).

The class of fiber reinforced concrete considered in the example is “3c” (MC2010), which is characterized by a characteristic flexural residual strength significant for serviceability conditions (f_{R1k}) equal to 3 MPa

and by a characteristic flexural residual strength significant for ultimate conditions (f_{R3k}) of 2.7 MPa.

The steel constituting reinforcing bars is characterized by a characteristic yield stress of 450 MPa (class “B450C” in the Italian national standard NTC2008 [9]) and by a modulus of elasticity of 210 GPa.

4.2 Constitutive laws used in the prediction

According to MC2010 (Figure 7.2-8 and Equations 7.2-13 and 7.2-14), a parabola-rectangle stress strain relationship is used for concrete in compression.

FRC in tension is modeled through two constitutive laws:

- a linear elastic – linear softening (le – ls) behavior;
- a bilinear hardening – bilinear softening (bh – bs) behavior.

As MC2010 classification of FRC is taken into account in this example, the constitutive laws proposed in MC2010 are used in the prediction of the channel behavior.

In the first case, the linear post-cracking stress-*CMOD* behavior is identified following the prescriptions proposed in Section 5.6.4 of MC2010 (linear model). In particular, it is defined through two points: ($0\text{ mm}; f_{Fts}$) and ($w_u; f_{Ftu}$) with:

$$f_{Fts} = 0.45 f_{R1}$$

$$f_{Ftu} = f_{Fts} - w_u/2.5 (f_{Fts} - 0.5f_{R3} + 0.2 f_{R1}) \quad (1)$$

w_u is limited to the minimum value between 2.5 mm and $l_{cs} \cdot \epsilon_{Fu}$ (where ϵ_{Fu} is the ultimate strain equal to 0.02 for variable strain distribution along the cross section and to 0.01 for constant tensile strain distribution along the cross section), MC2010- Section 5.6.4. The stress-strain relationship is obtained starting from the stress-*CMOD* curve by dividing the *CMOD* by the structural characteristic length, which varies according to the considered structural element portion.

In the second case, the bilinear hardening – bilinear softening stress-strain relationship is built following the prescription proposed in Section 5.6.5 of MC2010 (see Figure 5.6-11a).

In particular, the first, the second and the third branches are that of a plain concrete in uniaxial tension; the fourth branch (residual strength) is defined by two points corresponding to $(\varepsilon_{SLS}; f_{Fts})$ and $(\varepsilon_{ULS}; f_{Ftu})$, with f_{Fts} and f_{Ftu} determined as before and ε_{SLS} and ε_{ULS} determined as follow:

$$\begin{aligned} \varepsilon_{SLS} &= 0.5\text{mm} / l_{cs} \\ \varepsilon_{ULS} &= w_u / l_{cs} \end{aligned} \quad (2)$$

The maximum crack mouth opening displacement w_u is defined as before.

For each tensile constitutive relationship, the introduction of one or three characteristic lengths is taken into account.

When one characteristic length is introduced for the whole channel section, it can be computed as the minimum value between the mean distance between cracks s_{rm} and the distance y between the neutral axis and the tensile side of the cross-section (bent section). Hence, l_{cs} is chosen as the lower value between $y = 779$ mm and $s_{rm} = 224$ mm (which results equal to 224 mm). w_u results equal to 2.5 mm.

When three characteristic lengths are introduced, one characteristic length is defined for the channel vertical webs, one for the slab and one for the corner chords reinforced with traditional reinforcement.

The vertical webs are loaded in bending and are characterized by the presence of steel reinforcing bars concentrated in the bottom part of each web. Hence, for each web, the characteristic length can be defined as the distance y between the neutral axis and the tensile side of the L-shape bent section, which results equal to 663 mm.

The lower slab is loaded mainly in tension and does not present any traditional reinforcement. The material is softening in uniaxial tension and therefore the crack spacing is related to the slab width [2]; hence, the characteristic length is assumed equal to 1820 mm.

Considering the portion reinforced with traditional reinforcement, it is worth to note that this part is placed in the tensile zone of the element. The characteristic length can be

assumed equal to the average spacing between cracks in a reinforced concrete member subjected to tensile load. This average distance results equal to 84 mm.

w_u is defined in the three cases taking into account that the webs are bent, while the slab and the R/C parts are mainly loaded in tension. In particular, it results equal to 2.5 mm for the webs and the slab and to 0.84 mm for the reinforced R/C portions.

As suggested by MC2010 (Figure 7.2-15), an elastic-perfectly plastic behavior is assumed for steel in tension and compression.

4.3 Analytical results: longitudinal bending

Following a plane section approach, bending moment vs. curvature diagrams collected in Figure 7 are obtained considering both FRC tensile constitutive laws (le-ls and bh-bs) and both the cases in which one or three characteristic lengths are taken into account.

As a reference, a curve representing the cross-sectional behavior of a reinforced concrete U-section is plotted in the graph (dashed line). In this case the tensile strength of concrete is neglected.

All the curves are obtained considering characteristic material values.

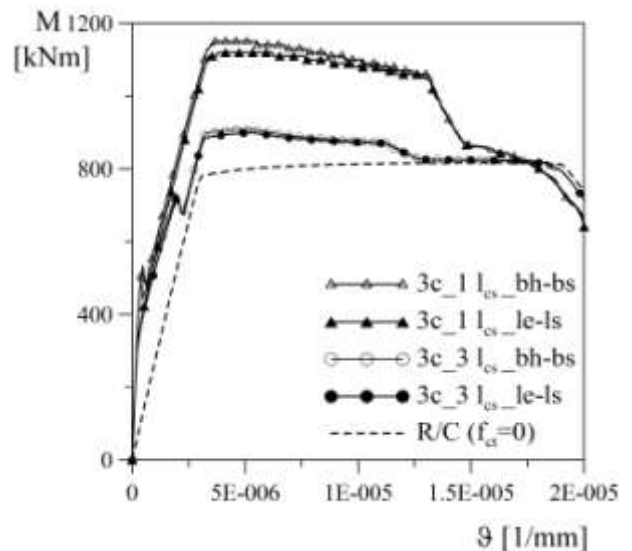


Figure 7: FRC class 3c sectional response: characteristic curves (three or one characteristic lengths; le-ls or bh-bs constitutive model) compared with the reference curve of R/C.

Looking at the figure it is possible to observe that, in this case, the use of one or three characteristic lengths results in a completely different sectional response, showing an overestimation of the maximum bending moment in case of adopting a unique characteristic length for the whole U-shaped section. The choice of using a more accurate FRC tensile constitutive law instead of the linear model does not give rise to a significant change in the global response of the element, thus indicating that the linear model approximation is enough for predicting the mechanical behavior of the FRC structure.

In order to better understand the obtained mechanical responses, they are plotted again in Figures 8 and 9, highlighting some relevant points on the curves. In particular:

- F1 means FRC cracking at the tensile side;
- F2 means reaching of the maximum tensile strength at the tensile side when a bilinear-hardening pre-pick behavior is assumed;
- S1 means rebar yielding (subscript “inf” refers to the inferior bars, and subscript “sup” refers to the upper bars);
- C1 means reaching of the maximum compressive strength (plateau) in concrete at the compressed side;
- C2 means concrete compressive failure at the compressed side;
- w_u indicates when an ultimate limit state is reached in FRC at the tensile edge (w_u refers to the case in which one characteristic length is used, while w_{u_lcs1} , w_{u_lcs2} and w_{u_lcs3} refer to the case in which three characteristic lengths are used and are related to the webs, the R/C portions and the slab respectively).

It is interesting to observe as in this case the reaching of the ultimate crack opening in the slab anticipates the steel yielding, due to the large value of the structural characteristic length. In the reality, the reaching of this limit does not involve a real collapse and therefore in this case the designer can renounce to the contribution of the bottom slab in tension, by continuing in

the curve at least up to the reaching of w_{u_lcs1} beyond which a soft softening takes place. If the designer is called to compute the ductility, the curve up to C2 limit can be considered.

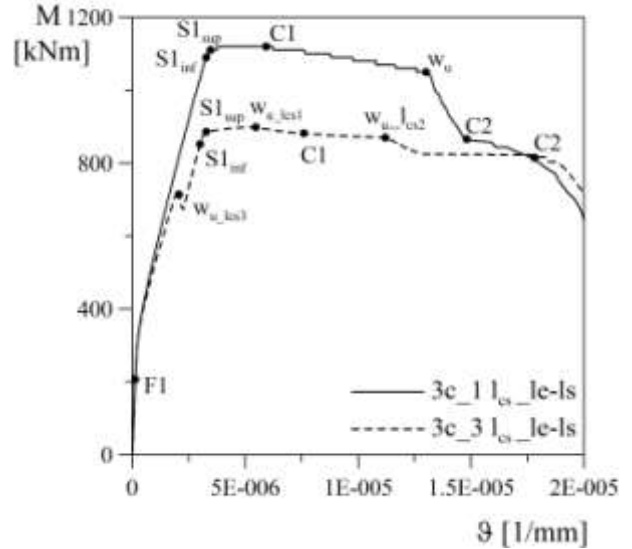


Figure 8: FRC class 3c sectional response: relevant points on characteristic curves obtained considering linear elastic - linear softening model.

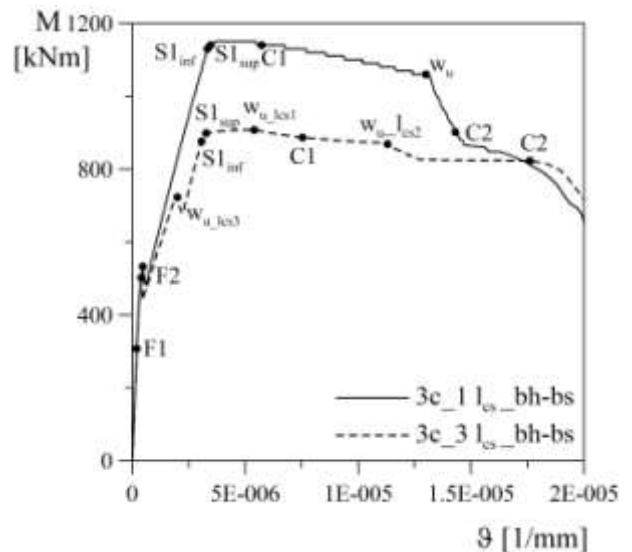


Figure 9: FRC class 3c sectional response: relevant points on characteristic curves obtained considering bi-linear hardening - bi-linear softening model.

4.4 Analytical results: transverse bending

As the section does not present transverse traditional reinforcement, the influence of fibers on the mechanical behavior is particularly important when transverse

bending is investigated.

The U-channel beam is characterized by two critical bent cross-sections in transverse direction: the base web section (considering each web as a cantilever beam) and the mid slab section.

As an example, the bent web section is investigated. As the section is under bending and there is no traditional reinforcement, the characteristic length is assumed equal to the thickness of the cross-section (MC2010 - Section 5.6.4).

The bending behavior is obtained assuming a width of 1 m, hence the responses shown in Figure 10 are plotted in terms of specific moment m versus curvature ϑ curves.

Also in this case characteristic curves are plotted for both FRC tensile constitutive laws (le-ls and bh-bs). The behavior of plain concrete is shown as a reference in the figure.

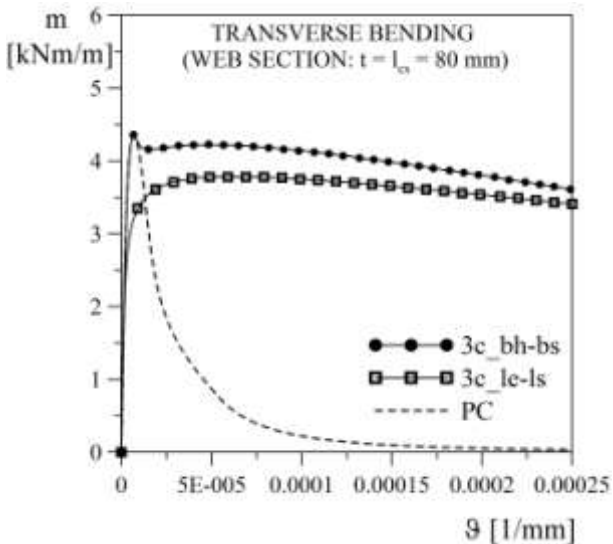


Figure 10: FRC class 3c sectional response for transverse bending: characteristic curves (le-ls or bh-bs constitutive model) compared with the reference curve of R/C.

Looking at the residual strength, the difference observed between the two curves “3c_le-ls” and “3c_bh-bs” is related to the FRC tensile relationships: the stress assumes a value equal to f_{Fts} for $w = 0$ mm in the first case, and for $w = 0.5$ mm in the second case.

5 U-CHANNEL: NUMERICAL MODEL

A 3D numerical model has been developed in the finite element program ABAQUS Standard 6.13. The element here studied is the same investigated in Section 4. In order to obtain the sectional response preventing shear failure, a four point load test on the beam is modeled, considering a lever arm equal to 9.92 m.

The U-shaped beam is modeled as a solid homogeneous section. Steel plates, also modeled as solid homogeneous sections, are added over the supports and under the loading knives in order to prevent any stress concentration and local failure of the element. Perfect bond is assumed between the bottom steel plates and the beam, while the top steel plates are free to move in tangential direction, in order to minimize strain concentration under the load application points.

Steel reinforcing bars are modeled through truss element embedded in the beam.

The beam and the steel plates are discretized with 8-node linear brick elements (C3D8R), and bars are discretized with 2-node linear 3-D truss elements (T3D2).

Just a quarter of the whole beam has been modeled, exploiting symmetries with respect to both x - y and y - z plane. The characteristics of the finite element mesh are collected in Table 4.

Table 4: FEM mesh characteristics.

Nodes (total number)	61666
Elements (total number)	43589
Elements type T3D2	1878
Elements type C3D8R	41711
Elements on the web thickness	2
Elements on the slab thickness	3
Max. aspect ratio (U-shaped beam)	1.13

The model geometry with constraints is shown in Figure 11, while the mesh is shown in Figure 12.

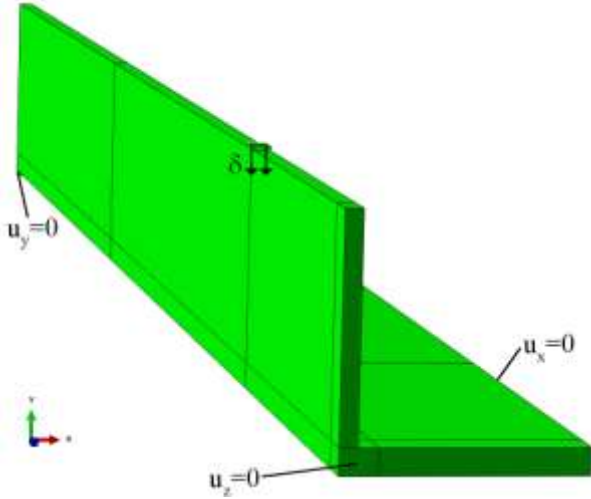


Figure 11: Finite element model: geometry with constraints.

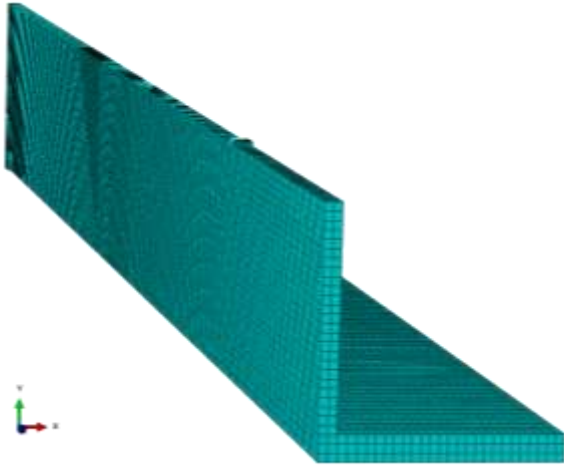


Figure 12: Finite element model: mesh.

5.1 Constitutive laws used in the model

The constitutive laws used in Abaqus finite element model for FRC section, steel rebars and steel plates are here summarized.

The elastic phase of fiber reinforced concrete is defined through two parameters:

- the Young's modulus, assumed equal to 35 GPa according to Table 1;
- the Poisson's ratio, assumed equal to 0.2.

Plasticity is introduced through Concrete Damage Plasticity model [10], which is implemented in Abaqus. Default plasticity parameters are used in the finite element analysis.

A parabolic-rectangular behavior is assumed for FRC in compression, with a

maximum strength f_{ck} equal to 35 MPa, reached at a strain equal to $2e-3$.

The plastic tensile behavior is defined introducing a bi-linear softening stress-displacement relationship. The first softening branch is that of a plain concrete class "C35" characterized by a maximum tensile strength f_{ctk} of 2.2 MPa. The second branch (residual strength) is defined by two points: $(0.5 \text{ mm}; f_{Fts})$ and $(2.5 \text{ mm}; 0.5 f_{R3} - 0.2 f_{R1})$. No maximum crack mouth opening displacement w_u is imposed.

The behavior of steel reinforcing bars is modeled through an elastic-perfectly plastic constitutive law, assuming a Young's modulus of 210 GPa and a yield strength of 450 MPa.

A linear-elastic behavior is assumed for steel plates used to prevent stress concentration.

5.2 Finite element model results

The numerical results obtained are shown in Figure 13 in terms of bending moment (M) versus curvature (ϑ) diagram. The curvature is computed as following:

$$\begin{aligned} \vartheta &= (\varepsilon_{inf} + \varepsilon_{sup}) / h \\ \varepsilon_{inf} &= \Delta u_{z_inf} / \Delta z \\ \varepsilon_{sup} &= \Delta u_{z_sup} / \Delta z \end{aligned} \quad (3)$$

with h height of the beam, Δz width of the beam portion across the crack that localizes and Δu_z elongation of the element edge. Subscript *inf* refers to the lower edge, while subscript *sup* refers to the upper edge of the beam portion.

The numerical response (dashed line) is stopped when the plastic strain of the lower edge on the beam portion considered to compute the curvature exceeds w_u / l_{cs} , computed in case of a unique characteristic length.

It is worth to note that the numerical curve is practically perfectly overlapped with the analytical response obtained using only one characteristic length. One of the reason is related to the small difference between the minimum characteristic tensile strength

(2.2 MPa) and the f_{Fts} one (= 1.35 MPa). This small difference induces also a reduced structural characteristic length, because the ratio between the two strengths is about 60% that means that only a part of the tensile force has to be transmitted from the reinforced chords to the bottom slab.

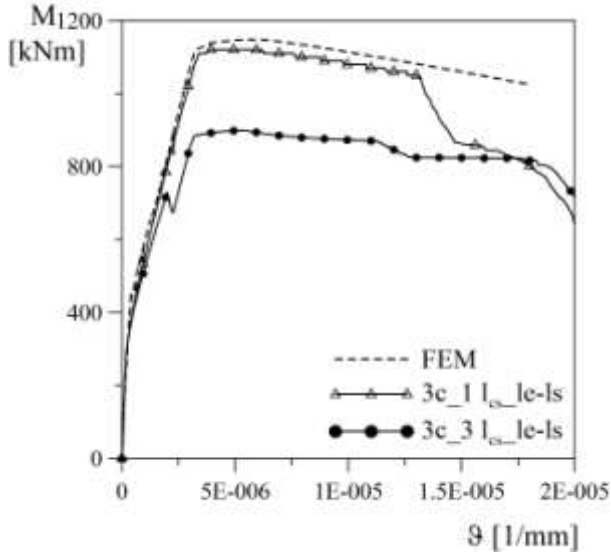


Figure 13: Finite element model results compared with analytical curves: bending moment vs. curvature diagram.

Another approximation is introduced by the formation of partial cracks, which are not at all considered in the plane-section model with different structural characteristic lengths, but that it could be often observed in real crack patterns. The crack pattern, developed according to F.E. analysis, is shown in Figure 14. It is interesting that integrating the plastic strains in the “grey” cracks a crack opening of about 2.4 mm can be computed, while it is only 0.4 mm in the “red” crack located between the previous ones. Another significant observation is that the automatic procedure introduced in the algorithm takes into account a characteristic length connected to the side length of each element, but in the macro-cracks the crack band extends to five elements, thus involving a spurious energy that significantly overestimates FRC contribution in tension. This numerical effect is related to the lack of a suitable calibration of the characteristic length that is affected by the

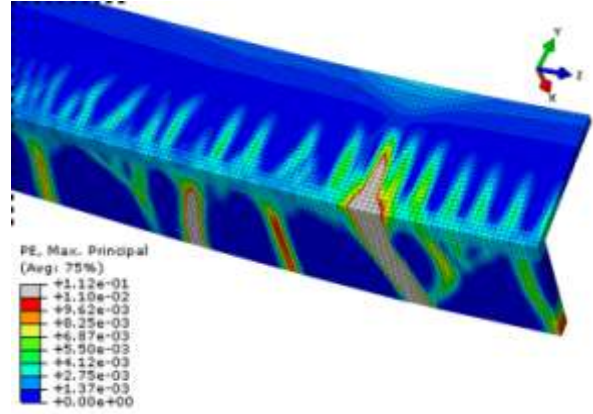


Figure 14: Finite element model results: plastic strain at the end of the numerical response.

class of the FRC investigated. It is also worth to note that in the analysis no damage was considered, thus reducing the energy release rate and thus stabilizing fictitiously the crack propagation.

6 CONCLUSIONS

Fiber reinforced concrete is characterized by a post-cracking residual strength that evolves with the crack opening. In order to conserve a smeared approach based on continuous strains, a structural characteristic length is required. This mechanical parameter depends on the kinematic model adopted.

Looking at a shallow beam where two cages located at the two edges scantily affect the computation of the characteristic length, because the reinforcement ratio is not homogeneous, but the variation in the width is limited, both the plane-section models assuming one or two characteristic lengths give similar predictions.

Looking at a thin-walled FRC U-channel, two extreme conditions are investigated by using a plane-section approach and then compared with a Finite Element investigation.

The results highlight a significant difference in the predicted behavior: the solution with three different lengths exhibits the lowest bearing capacity in bending (about -25%), while Finite Element investigation gives the highest value, scantily higher than that predicted by plane-section approach, when a

unique characteristic length is considered. The different bearing capacity is mainly affected by the correct prediction of crack spacing and a suitable calibration of the crack band width that has not to introduce a spurious energy.

REFERENCES

- [1] Leonhardt, F. 1987. Cracks and crack control at concrete structures. In *IABSE proceedings P-109/87, IABSE PERIODICA 1/1987*; pp. 25-44.
- [2] di Prisco, M., Iorio, F., and Plizzari, G. 2003. HPSFRC prestressed roof elements. In Schnütgen, B., and Vandewalle, L. (Eds), *Test and design methods for steel fibre reinforced concrete – Background and experiences PRO 31, RILEM*; pp. 161-188.
- [3] Zani, G. 2013. *High Performance Cementitious Composites for Sustainable Roofing Panels*. PhD thesis, Doctoral School in Structural, Seismic and Geotechnical Engineering, Politecnico di Milano.
- [4] di Prisco, M., Colombo, M., Bonalumi, P., and Beltrami, C. 2014. FRC structural applications according to model code 2010: a unified approach. In Charron, J.P., Massicotte, B., Mobasher, B., and Plizzari, G. (Eds) *Proceedings of the FRC 2014 Joint ACI-fib International Workshop “Fibre Reinforced Concrete: from Design to Structural Applications”*.
- [5] *fib Model Code for Concrete Structures 2010*. Published by Ernst & Sohn (2013).
- [6] European standard EN 14651: 2005 - Test method for metallic fibre concrete - Measuring the flexural tensile strength (limit of proportionality (LOP), residual).
- [7] European standard EN 1990: 2002 - Eurocode - Basis of structural design.
- [8] di Prisco, M., Colombo, M., and Dozio, D. 2013. Fibre-reinforced concrete in fib Model Code 2010: Principles, models and test validation. *Structural Concrete* 14: 342-361.
- [9] Italian standard NTC 2008 - Norme tecniche per le costruzioni.
- [10] Lee, J., and Fenves, G. 1998. Plastic-Damage Model for Cyclic Loading of Concrete Structures. *Journal of Engineering Mechanics*, 124(8):892-900.
- [11] Ferrara, L., di Prisco, M. 2001. Mode I fracture behavior in concrete: Nonlocal damage modeling, *Journal of Engineering Mechanics*, 127 (7), pp. 678-692.